

SPADA: A Spatial Dataflow Architecture Programming Language

Lukas Gianinazzi
 Noéda, ETH Zurich
 Zurich, Switzerland
 lux@noeda.ai

Tal Ben-Nun
 Lawrence Livermore National Laboratory
 Livermore, California, USA

Torsten Hoefer
 Department of Computer Science
 ETH Zurich
 Zurich, Switzerland

Abstract—Spatial dataflow architectures like the Cerebras Wafer-Scale Engine achieve exceptional performance in AI and scientific applications by leveraging distributed memory across processing elements (PEs) and localized computation. However, programming these architectures remains challenging due to the need for explicit orchestration of data movement through reconfigurable networks-on-chip and asynchronous computation triggered by data arrival. Existing FPGA and CGRA programming models emphasize loop scheduling but overlook the unique capabilities of spatial dataflow architectures, particularly efficient dataflow over regular grids and intricate routing management.

We present SPADA, a programming language that provides precise control over data placement, dataflow patterns, and asynchronous operations while abstracting architecture-specific low-level details. We introduce a rigorous dataflow semantics framework for SPADA that defines routing correctness, data races, and deadlocks. Additionally, we design and implement a compiler targeting Cerebras CSL with multi-level lowering.

SPADA serves as both a high-level programming interface and an intermediate representation for domain-specific languages (DSLs), which we demonstrate with the GT4Py stencil DSL. SPADA enables developers to express complex parallel patterns—including pipelined reductions and multi-dimensional stencils—in 6–8× less code than CSL with near-ideal weak scaling across three orders of magnitude. By unifying programming for spatial dataflow architectures under a single model, SPADA advances both the theoretical foundations and practical usability of these emerging high-performance computing platforms.

I. INTRODUCTION

A. Motivation

Spatial dataflow architectures (SDAs) have emerged as powerful platforms for achieving exceptional performance in latency-sensitive applications, including neural network inference and stencil-based physical simulations used in weather forecasting and computational fluid dynamics. These architectures excel by leveraging high local memory throughput and localized processing, positioning them as strong contenders in high-performance computing (HPC) [13], [15].

The key to their high memory throughput lies in memory disaggregation, distributed across processing elements (PEs). Unlike traditional architectures with shared global memory and complex cache hierarchies, spatial dataflow architectures eliminate cache management entirely, using only fast localized SRAM within each PE. This configuration drastically reduces local memory access latency to sub-nanosecond levels and

avoids shared memory contention overhead, achieving memory bandwidth that conventional systems cannot match.

However, the absence of shared memory introduces significant programming challenges. Data movement between PEs must be explicitly orchestrated using reconfigurable circuits controlled by routers in the network-on-chip (NoC). Computations are triggered asynchronously as data arrives, requiring careful synchronization across the distributed fabric. Furthermore, the circuit-switched network provides only a limited number of concurrent communication channels, necessitating explicit channel assignment to avoid routing conflicts. As a result, programming SDAs for large-scale applications becomes time-intensive and error-prone. Routing conflicts and data races manifest non-deterministically at runtime across distributed hardware, making debugging particularly arduous. These programming barriers prevent the HPC community from fully exploiting these architectures’ performance capabilities.

B. Limitations of State-of-the-Art

Previous work for spatial architectures has focused on FPGA and CGRA programming models that emphasize loop scheduling techniques such as tiling, unrolling, pipelining, and parallelization to optimize computational throughput [6]. However, FPGAs lack the hardened processing elements present in spatial dataflow architectures—coarse-grained compute units that follow a von Neumann architecture. More critically, FPGA tools assume packet-switched networks with dynamic routing, whereas spatial dataflow architectures use circuit-switched networks requiring explicit channel assignment to prevent routing conflicts. These fundamental differences mean FPGA programming models overlook two critical aspects of SDAs: efficient handling of spatial dataflow and routing configuration.

While spatial dataflow architectures are increasingly used in domains such as physical simulations [5], [12], [22] and machine learning [8], [23], existing approaches rely on tailor-made communication patterns [16], [20] and lengthy low-level codes tightly coupled to specific algorithms. These approaches are limited to specific domains and lack the generality needed for broader applications. Our work addresses this gap by introducing a unifying programming model that supports a wide range of applications and can also serve as an intermediate language for domain-specific languages (DSLs), thereby enabling productive programming in fields like weather forecasting.

C. Methodology

To achieve high performance on spatial dataflow architectures, our approach allows programmers to explicitly specify data partitioning and dataflow patterns. Rather than exposing low-level task graphs and data-triggered execution models, we provide high-level asynchronous constructs: `async-await` for dependency management, asynchronous `foreach` loops over data streams, and `map` scopes for vectorized operations. These abstractions give programmers intuitive control over synchronization while hiding underlying complexity.

Communication relies on circuit-switched networks with limited concurrent channels. While our language requires explicit stream declarations, we automate channel assignment through a semantic framework that defines correctness conditions for routing conflicts and execution order. Our checkerboard decomposition algorithm guarantees conflict-free allocation by construction, transforming routing from a runtime into a compile-time problem.

This methodology—explicit dataflow control through high-level abstractions combined with automated resource management—enables the insights and contributions that follow.

D. Key Insights and Contributions

Our work advances both the practical and theoretical foundations for programming spatial dataflow architectures.

Language Design. We introduce SPADA, a programming language that provides explicit control over data placement, dataflow patterns, and asynchronous execution while abstracting architecture-specific routing details. SPADA enables expressing complex spatial algorithms—including multi-dimensional stencil computations and collective communication primitives—succinctly without sacrificing performance-critical design choices. The language serves dual roles: as a direct programming interface for expert users and as a compiler intermediate representation for domain-specific frontends like GT4Py, enabling domain scientists to target spatial architectures through familiar interfaces.

Dataflow Semantics. We present a semantical framework that defines correctness for routing configurations on spatial dataflow architectures. This formalization enables reasoning about data races and routing conflicts. The framework provides the foundation for our routing assignment algorithm.

Automatic Routing Assignment. We develop a checkerboard decomposition algorithm that guarantees conflict-free channel assignment by construction. The algorithm exploits spatial regularity in communication patterns to partition PE grids such that messages from different sources cannot physically interfere, then assigns separate channels to these partitions. This eliminates the manual reasoning required to assign communication streams to limited hardware channels, making spatial dataflow programming more accessible without requiring deep hardware expertise.

End-to-End Compilation. We implement a complete compilation pipeline from GT4Py—a production stencil DSL used for weather forecasting—to Cerebras CSL. The pipeline introduces a Stencil IR that decouples domain-specific semantics

from spatial architecture lowering, then performs multi-stage transformation through canonicalization, routing assignment, task decomposition, and code generation with automatic vectorization. This implementation validates SPADA’s viability as both a programming language and compiler target.

Experiments. We evaluate SPADA on a Cerebras WSE-2 with three hand-written kernels and three stencil computations. Our results demonstrate that SPADA reduces code size by 6–8 \times compared to hand-written CSL for algorithmic kernels, and by up to 700 \times when lowering from GT4Py stencils. The compiler-generated code achieves over 150 TFlop/s on complex momentum equation kernels and exhibits near-ideal weak scaling across three orders of magnitude in problem size.

E. Limitations

SPADA establishes foundational programming abstractions for spatial dataflow architectures. Our compiler provides a foundational set of optimizations, leaving room for future improvements. Our automatic routing assignment handles common communication patterns for stencils and communication collectives; more complex patterns may be specified manually. By providing principled abstractions and automated resource management, SPADA creates a platform for systematic performance improvements and expanded application support.

II. CEREBRAS WAFER-SCALE ENGINE AND CSL

The Cerebras Wafer-Scale Engine (WSE) comprises hundreds of thousands of processing elements (PEs) arranged in a two-dimensional grid. Each PE contains local SRAM and an ALU optimized for floating-point operations. Unlike cache-based architectures, the WSE achieves high throughput through disaggregated memory—each PE accesses only its local memory with sub-nanosecond latency. Programming the WSE is accomplished through the Cerebras Software Language (CSL), a low-level kernel language that provides explicit control over communication, memory, and task scheduling.

Circuit-Switched Communication. PEs communicate through a circuit-switched network-on-chip where data packets called *wavelets* traverse configured routing paths. Each router supports a limited number of concurrent circuits, identified by *colors* in CSL terminology, which are virtual communication channels bound to physical routing resources. Concurrent communication streams must be assigned distinct colors to avoid routing conflicts. Unlike packet-switched networks, the circuit-switched fabric requires explicit routing configuration and channel assignment. Colors are limited resources (24 per PE, and 8 reserved), requiring judicious allocation.

Task-Driven Execution. Computation follows an asynchronous task model where *local tasks* are activated programmatically and *data tasks* trigger automatically upon wavelet arrival. A task runs only when both *active* and *unblocked*, with explicit `@activate` and `@unlock` operations enabling fine-grained synchronization. As with colors, task identifiers are also limited resources: up to 28 per PE, which cannot overlap with colors, reducing the effective count.

Vectorized Operations. High performance on the WSE requires exploiting hardware-accelerated vectorized operations through *Data Structure Descriptors* (DSDs). DSDs encode memory access patterns and fabric communication routes, enabling single-instruction operations like `@fadd`, `@fmul`, and `@fmac` to process entire arrays. Expressing computations as DSD operations rather than scalar loops is crucial for achieving peak PE utilization.

III. SPADA LANGUAGE DESIGN

Our language framework enables precise control over data placement, data movement, and asynchronous execution, essential for programming spatial dataflow architectures effectively. This section introduces the main constructs: `place` blocks for data allocation across processing elements (PEs), `dataflow` blocks for setting up communication streams, and `compute` blocks for defining operations on both streamed and locally stored data. Table I provides a brief reference of the language constructs available within these blocks.

Each block is defined for some *subgrid*, which is specified using a range expression for each dimension. In the example `place i32 i, i32 j in [0:I:2, 1:J-1] { ... }`, the variables `i` and `j` represent the coordinates of each PE in the subgrid $[0:I:2, 1:J-1]$, which covers every second PE in the first dimension (with a stride of 2) from 0 to I and every PE in the second dimension from 1 to $J - 2$ (exclusive).

Blocks can be organized into *phases*, which serve as local scopes. Routing declarations and data allocated within a phase are only accessible within that specific phase. From the perspective of each processing element (PE), phases execute sequentially in the order they are defined in the code. However, phase transitions occur asynchronously across PEs, allowing one PE to move to the next phase even if other PEs are still completing the current one.

Together, these constructs provide a programming model that balances low-level control with high-level abstraction, allowing developers to write efficient, high-performance programs tailored to spatial architectures. We now examine each of the three block types in more detail.

A. Place Blocks

The `place` block specifies where data is stored across the grid of processing elements (PEs). Within a `place` block, developers can allocate local data elements—either scalars or arrays—that are assigned to specific PEs based on their coordinates in a defined subgrid. Arrays and scalars contain undefined values upon initialization. Each `place` block defines memory allocations for the specified subgrid, forming a data layout across the processing grid. This layout ensures efficient data access for subsequent computations by placing data close to the PEs that will process it.

B. Dataflow Blocks

The `dataflow` block defines communication streams between PEs, establishing virtual data channels through which

information flows. Each stream follows a relative communication pattern, meaning that connections are defined by offsets relative to each PE’s position in the subgrid. In particular, the declaration `stream<f32> s = relative_stream(x, y)` declares a stream that sends data from a PE at coordinate (i, j) to a PE at coordinate $(i + x, j + y)$. If the stream is used for receiving, a PE at coordinate (i, j) receives data from a PE at coordinate $(i - x, j - y)$. This implicit swapping of directionality when sending and receiving on the same stream enables pipelined communication chains, as seen in Listing 1.

Each stream name must be unique within a `dataflow` block. Additionally, streams can be configured with specific routing paths and channel assignments, providing precise control over data movement while managing limited hardware resources on the circuit-switched network.

Routing Declarations: Optionally, a routing declaration may be set up for each stream. This declaration describes how the data is routed between the PEs. Specifically, for each stream, the configuration can specify intermediate hops that the data takes. Additionally, a `channel`, which represents a limited hardware resource (either virtual or hardware-based), can be specified to route the data efficiently. The routing configuration is set up as follows:

```
stream<T> stream_name = relative_stream(dx, dy) {
    hops = [(dx_1, dy_1), ..., (dx_n, dy_n)],
    channel = channel_id
}
```

Here, `hops` is a list of relative hops that the data takes between the sender and receiver, where each hop is specified by a pair of constant literals whose sum of absolute values must equal 1. The sum of all hops must match the relative position of the stream. If two messages (elements of a `send`) are routed through a PE simultaneously, it is essential to ensure that they do not share the same `channel`.

C. Compute Blocks

The `compute` block defines the computations executed by each PE. Computations may be triggered by incoming data from streams, and can be asynchronous. This allows operations to overlap with data movement and thus minimizing idle time. Asynchronous constructs like `send`, `receive`, and `foreach` enable a data-driven model where computations adapt to the dynamic flow of information across the grid.

To manage execution order and dependencies, *completions* are used. Completions track the status of asynchronous tasks and ensure that each operation either has a unique completion assigned or is prefixed with `await`. The `await` operation synchronizes tasks by blocking until a specified completion is triggered or prefixed operation completes. For instance, `await send(a, s)` ensures that the `send` operation finishes before moving to the next operation and `await c` for some completion `c` ensures that the operation associated with `c` has completed before the next operation starts.

Note that a `send` operation completes once the send buffer may be safely overwritten, not when the receiver has received

TABLE I
CORE SPADA LANGUAGE CONSTRUCTS

Construct	Description
<code>phase { ... }</code>	Wraps a set of blocks to declare a scope.
Within a <code>place</code> block: <code>T scal / T[...] arr</code>	Declares a local scalar or (multidimensional) array of type T
Within a <code>dataflow</code> block: <code>stream<T> s = relative_stream(dx, dy)</code>	Declares a stream s of element type T
Within a <code>compute</code> block: <code>send(a, s)</code> <code>foreach f32 x in receive(s) { ... }</code> <code>foreach u16 k, f32 x in [0:J], receive(s) { ... }</code> <code>map i32 i in [I:J:K] { ... }</code> <code>async { ... }</code> <code>completion c = ...</code> <code>await c</code> <code>awaitall</code> <code>for i64 i in [I:J:K] { ... }</code>	Asynchronously sends array a over stream s Iterates over each element received from the stream s Iterates over an element range received from stream s Asynchronous parallelizable <i>affine</i> loop Creates an asynchronous block of code Get a completion handle for an asynchronous operation Waits for a specified completion c before proceeding with further computation Waits for all pending completions before proceeding Synchronous sequential loop

the data. Any completion not explicitly awaited is automatically awaited at the end of the `compute` block, guaranteeing that all tasks complete before the block exits. We implicitly add an `awaitall` operation for all completions at the end of each `compute` block, locally synchronizing all pending operations before moving to the next phase.

An operation that must complete before any subsequent operation can start is termed a *blocking operation*. In particular:

- `await` statements are blocking, including asynchronous operations that immediately await their completion.
- Assignments to fields are blocking.
- For loops are blocking.

We impose the following restrictions to ensure that communication sites are deterministic: if communication occurs, it always involves the same predetermined PEs and operations.

- Within each `compute` block, correctly synchronized `send` operations to the same stream execute in local order.
- Asynchronous statements within loops must be explicitly awaited inside the loop.
- Every `send` operation within a loop or conditional block must have a corresponding `receive` operation within each receiving `compute` block, i.e., it is disallowed to receive or send over the same stream in both branches of an `if-else`.

As we shall show in Section IV, by enforcing these constraints, we prevent ambiguous communication patterns and enable a straightforward and unambiguous semantics.

This asynchronous model allows operations to be preempted and interleaved, maximizing parallelism and compute/communication overlap. By explicitly managing dependencies with `await`, data races can be avoided, ensuring predictable execution across PEs. The combination of `place`, `dataflow`, and `compute` blocks provides fine-grained control over data placement, movement, and processing on spatial architectures.

D. Example: 1D Pipelined Reduce

The kernel in Listing 1 performs a 1D pipelined reduction across a row of processing elements (PEs), outputting the

```

kernel @pipelined_reduce<K> (stream<f32>[K] readonly a_in,
                             stream<f32>[1] writeonly out) {
    place i16 i, i16 j in [0:K, 0] {
        f32[K] a
    }
    // Phase 1: Read argument stream
    phase {
        compute i32 i, i32 j in [0:K, 0] {
            await receive(a, a_in[i])
        }
    }
    // Phase 2: Perform reduction
    phase {
        // Declare dataflow
        dataflow i32 i, i32 j in [0:K, 0] {
            stream<f32> red = relative_stream(-1, 0)
            stream<f32> blue = relative_stream(-1, 0)
        }
        // East corner
        compute i32 i, i32 j in [K-1, 0] {
            await send(a, red if (N-1) % 2 == 0 else blue)
        }
        // Odd PEs
        compute i32 i, i32 j in [1:K-1:2, 0] {
            await foreach i32 k, f32 x in [0:K], receive(red) {
                a[k] = a[k] + x
                await send(a[k], blue)
            }
        }
        // Even PEs
        compute i32 i, i32 j in [2:K-1:2, 0] {
            await foreach i32 k, f32 x in [0:K], receive(blue) {
                a[k] = a[k] + x
                await send(a[k], red)
            }
        }
        // West corner (root)
        compute i32 i, i32 j in [0, 0] {
            await foreach i32 k, f32 x in [0:K], receive(blue) {
                a[k] = a[k] + x
            }
            await send(a, out[i])
        }
    }
}

```

Listing 1: SPADA 1D Pipelined Reduction Kernel

result at the west-most PE. This reduction is implemented in two phases: (1) data loading and (2) the pipelined reduction, followed by a final output transmission.

The initial `place` block allocates a local array `a` of type `f32[K]` at each PE. In the data-loading phase, each PE

asynchronously receives data from the input stream `a_in`, initializing the array `a` for further computation.

The pipelined reduction phase uses alternating red and blue streams. Using two streams ensures that no PE attempts to send and receive from the same stream simultaneously. The pipelined approach minimizes contention and is very efficient for large vector sizes [16]. Using two streams ensures that no PE attempts to send and receive from the same stream simultaneously, which would otherwise cause communication conflicts and undefined behavior. This double-buffered strategy effectively maintains data flow without interruptions. In detail, the reduction proceeds as follows:

East Corner: The eastmost PE sends its data on either the red or blue stream, depending on its position.

Odd and Even PEs: Intermediate PEs alternate between receiving data, accumulating it into their local array `a`, and forwarding the result, thereby realizing an efficient pipeline.

West Corner: The westmost PE completes the reduction by receiving the final segment, performing the last accumulation, and sending the result to the output stream `out`.

In summary, this kernel demonstrates how our language's constructs enable efficient pipelined reductions by providing explicit control over data movement and computation.

E. Discussion

Our approach equips developers with precise control over dataflow, data placement, and asynchronous execution on spatial dataflow architectures. This programming model is particularly well-suited for applications requiring fine-grained control over data movement and processing, such as scientific computing, machine learning, and large-scale simulations. The explicit handling of data placement and communication enables fully exploiting the underlying hardware's capabilities without low-level routing and synchronization, achieving both improved performance and productivity.

IV. SEMANTICS

Programming spatial dataflow architectures requires reasoning about asynchronous execution across distributed PEs with explicit routing through circuit-switched networks. Unlike packet-switched systems where prior semantic frameworks apply [4], [9], [11], spatial dataflow architectures demand semantics that capture deterministic routing paths and limited physical channels—properties that enable stronger correctness guarantees but require new formal treatment.

SPADA's asynchronous constructs (`async-await`, `foreach`, `map`) permit arbitrary operation interleaving for performance, creating three correctness challenges: (1) non-deterministic local execution ordering within PEs, (2) concurrent access to shared resources including memory and communication channels, and (3) distributed data dependencies spanning multiple PEs. Without formal semantics, these manifest as data races, deadlocks, and routing conflicts that appear non-deterministically at runtime—precisely the issues SPADA aims to address.

We present a semantic framework with two key abstractions: *stream edges* representing communication dependencies, and *routing graphs* modeling physical data paths with channel assignments. These abstractions enable us to define precise correctness conditions: a routing configuration is valid if concurrent communications never share channels on overlapping paths. This formalization provides the foundation for our automatic routing assignment algorithm (Section VI-B), transforming routing correctness from a runtime property into a compile-time guarantee. The semantics thus bridges SPADA's high-level programming model with the low-level constraints of spatial dataflow hardware.

A. Execution Model

We adapt standard concurrency theory [1], [14], [17] to spatial dataflow architectures.

a) Happens-Before: For operations S_1 and S_2 at PEs (i_1, j_1) and (i_2, j_2) , we write $S_1, (i_1, j_1) \rightarrow S_2, (i_2, j_2)$ if every instance of S_1 completes before the corresponding instance of S_2 starts. When this holds for all PEs in the subgrid, we write $S_1 \rightarrow S_2$ for brevity. This *happens-before* relation specifies execution order across the distributed system.

b) Concurrency: Operations S_1 and S_2 are *concurrent* if there exist PEs (i, j) and (i', j') such that neither $S_1, (i, j) \rightarrow S_2, (i', j')$ nor $S_2, (i', j') \rightarrow S_1, (i, j)$ holds.

c) Local Order: The *local order* $S_1 \preceq S_2$ defines sequential execution within a single PE's compute block. We say S_2 follows S_1 in local order if S_2 syntactically follows S_1 on all execution paths and either (1) S_1 is a blocking operation, or (2) S_1 is non-blocking with completion `c` and an `await c` appears on all paths before S_2 .

d) Data Race: A *Data Race* occurs if a operation writes to an array element while another concurrently reads from or writes to it on the same PE. Data races lead to undefined behavior. To prevent data races, one must synchronize `send` and `receive` operations with `await` as needed. This strict rule ensures determinism regardless of the interleaving of concurrent operations.

e) Deadlock: Some asynchronous statements cannot make progress until some event occurs. In particular, a `foreach` stalls until the next element is received, and each `await` stalls until the corresponding completion triggers. A `send` stalls while the receiver is not ready to receive the data. It is guaranteed that if there exists a statement that can make progress, at least one of them will make progress. However, SPADA does not guarantee fairness, that is, concurrent statements may be executed in any respective order and may be preempted at any time. Failure to guarantee completion regardless of progress order of concurrent operations constitutes a *deadlock*. Proper synchronization and ordering of asynchronous operations ensure deadlock-free execution.

B. Communication Model

Intuitively, a stream edge represents a point-to-point communication link created when one PE sends data that another PE receives. These edges form the backbone of our dataflow

programs, determining both the flow of data and the synchronization constraints between operations. These edges connect `send` and `receive` operations across different PEs, ensuring data flows correctly through the network.

Formally, a *stream edge* exists from $(S_1, (i_1, j_1))$ to $(S_2, (i_2, j_2))$ if data sent by the operation S_1 at PE (i_1, j_1) is received by the operation S_2 at PE (i_2, j_2) . This establishes a communication link between the source and destination PEs.

The following conditions ensure that stream edges are always uniquely and deterministically defined: Within each compute block, correctly synchronized `send` operations *to the same stream* execute in local order. Additionally, each asynchronous statement within a loop must be awaited inside the loop. Finally, every `send` operation nested in a loop or `if-else` must correspond to exactly one `receive` operation nested in a loop or `if-else` within each receiving compute block. In particular, it is disallowed to send or receive over the same stream in both branches of an `if-else`.

These conditions allow for data-dependent communication, but restrict each stream’s usage to ensure that if communication does occur, it is deterministic—always involving the same predetermined PEs and operations.

C. Routing Model

Circuit-switched networks have limited channels that cannot be shared by concurrent communications. This section formalizes which routing declarations correctly respect these hardware constraints.

a) *Strict Happens-Before Relation*: We define a *strict happens-before* relation that strengthens the happens-before relation and is essential for interpreting routing declarations and their correctness. Statement S_1 at PE (i_1, j_1) *strictly happens-before* statement S_2 at PE (i_2, j_2) (denoted as $S_1, (i_1, j_1) \rightarrowtail S_2, (i_2, j_2)$) if all instances of S_1 complete at PE (i_1, j_1) before the first instance of S_2 begins at PE (i_2, j_2) .

b) *The Routing Graph*: The *routing graph* of a phase is a directed graph that describes how data is routed between PEs. This graph is defined in terms of PE coordinates. The routing graph consists of the following elements: Each PE is a vertex. For each stream edge from PE (x_1, y_1) to PE (x_2, y_2) over stream F on channel C , using intermediate hops $[(dx_1, dy_1), \dots, (dx_n, dy_n)]$, we add edges between these intermediate PEs. Each path is recorded along with its stream, channel, and corresponding stream edge.

c) *Channel Conflicts and Undefined Behavior*: We can characterize the correctness conditions on routing declarations using the routing graph and the following notion on the ordering of stream edges: A stream edge $(S_1, (i_1, j_1), S_2, (i_2, j_2))$ *empties-before* another stream edge $(S_3, (i_3, j_3), S_4, (i_4, j_4))$ if $S_2, (i_2, j_2) \rightarrowtail S_3, (i_3, j_3)$.

If two paths in the routing graph use the same channel, share a PE, and their corresponding stream edges are not ordered by *empties-before*, *the behavior is undefined*. This condition ensures that messages do not interfere with each other, maintaining deterministic circuit-switched routing. Sending data

through the same stream in the same phase is allowed as long as sends and receives are properly synchronized.

V. STENCIL DSL FRONTEND

SPADA serves as both a programming language and a compiler intermediate representation. We demonstrate the latter by implementing a complete compilation pipeline from GT4Py, a production stencil DSL used for weather and climate modeling, to executable code on the Cerebras WSE.

GT4Py [3], [21] is a production embedded Python DSL used by CSCS and MeteoSwiss for weather forecasting. It allows domain scientists to express stencil computations using intuitive syntax. Listing 2 shows a Laplacian in GT4Py:

```
@stencil
def laplace(in_field: Field3D, out_field: Field3D):
    with computation(PARALLEL), interval(...):
        out_field = -4.0 * in_field[0, 0, 0] +
                    in_field[1, 0, 0] + in_field[-1, 0, 0] +
                    in_field[0, 1, 0] + in_field[0, -1, 0]
```

Listing 2: Laplacian in GT4Py

This specification abstracts away data distribution, communication patterns, and synchronization. Direct lowering to SPADA is challenging because GT4Py’s domain-specific semantics (iteration intervals, vertical strategies, boundary conditions) don’t map cleanly to SPADA’s explicit PE-level programming model.

We introduce a *Stencil IR* that captures: (1) which field accesses require inter-PE communication versus local computation, (2) what halo regions boundary PEs need to satisfy neighbor dependencies, and (3) the data types and iteration domains for all operations. This intermediate representation decouples high-level stencil semantics from spatial code generation, enabling reuse across multiple stencil frontends and architecture-independent optimizations.

The Stencil IR is lowered to SPADA through three simultaneous passes. The *placement pass* allocates local arrays on each PE based on computed field sizes and halos. The *dataflow pass* identifies communication patterns from stencil access offsets and generates stream declarations—for the Laplacian, the four neighbor accesses at offsets $(\pm 1, 0, 0)$ and $(0, \pm 1, 0)$ become four `relative_stream` declarations. The *compute pass* transforms each stencil statement into SPADA operations, inserting `send/receive` pairs where neighbor data crosses PE boundaries and generating `map` operations for local computation. Rectangle splitting and merging algorithms coalesce operations with identical subgrids, reducing code duplication.

VI. CSL COMPILER BACKEND

Lowering SPADA to executable Cerebras CSL code requires bridging a fundamental abstraction gap: SPADA expresses computations over logical PE grids with abstract communication streams, while CSL demands explicit hardware task graphs, data structure descriptors (DSDs), and physical routing configurations. This transformation must preserve SPADA’s

asynchronous semantics while exploiting CSL’s hardware-accelerated primitives—vectorized DSD operations, wavelet-triggered tasks, and circuit-switched fabric communications.

We implement a multi-stage compilation pipeline that systematically lowers SPADA’s high-level constructs to CSL’s architecture-specific features. (1) Canonicalization normalizes SPADA into standard form with unique files for each PE type. (2) Routing assignment guarantees conflict-free channel allocation through checkerboard decomposition, producing routed SPADA. (3) Task assignment extracts completion DAGs and coarsens them into CSL tasks, whether user- or wavelet-triggered. (4) Code generation synthesizes DSD-optimized CSL code with pattern matching. (5) I/O mapping configures CSL memory layouts and communication modes. We now detail each stage.

A. Canonicalization

The lowering process begins with passes that normalize SPADA into a form amenable to hardware mapping. These passes: (a) consolidate rectangles into *PE equivalence classes* mapped to non-overlapping strided regions, ensuring each PE corresponds to a single CSL code file; (b) unify `phase` blocks with `awaitall` synchronization markers, standardizing each subgrid to contain exactly one `place`, `dataflow`, and `compute` block; and (c) decompose high-level array operations on fields into explicit `foreach` or `map` blocks with index calculations.

B. Automatic Routing Assignment

While canonicalization follows standard compiler techniques, the subsequent routing assignment stage addresses a challenge unique to spatial dataflow architectures: *automatic channel allocation with conflict avoidance*. When multiple data streams traverse shared physical routing resources, they must be assigned to distinct channels to prevent race conditions and undefined behavior. We solve this through a checkerboard decomposition algorithm (Figure 1) that guarantees conflict-free routing by construction, eliminating the error-prone manual reasoning required in prior WSE implementations.

Our current implementation restricts streams to single-hop communication ($\|dx\| + \|dy\| \leq 1$), which suffices for all weather stencils in our evaluation (Section VII). The algorithm can be extended to deal with multi-hop scenarios.

Checkerboard Decomposition. We first identify *active dimensions*: a dimension is active if any stream has non-zero offset in that dimension. Each `compute` block is then split based on PE coordinate parity into 2 blocks for each active dimension. Each stream `s` is duplicated into `s_even` and `s_odd`. The key insight is that messages from even-coordinate PEs travel only through even-coordinate intermediate PEs, while messages from odd-coordinate PEs traverse only odd-coordinate PEs. This eliminates all routing conflicts.

At each `send` or `receive` operation on stream `s = relative_stream(dx, dy)`, we replace `s` with either `s_even` or `s_odd` as described in Listing 3. We assign each resulting unique stream a distinct channel identifier. The checkerboard construction guarantees that streams sharing a channel never

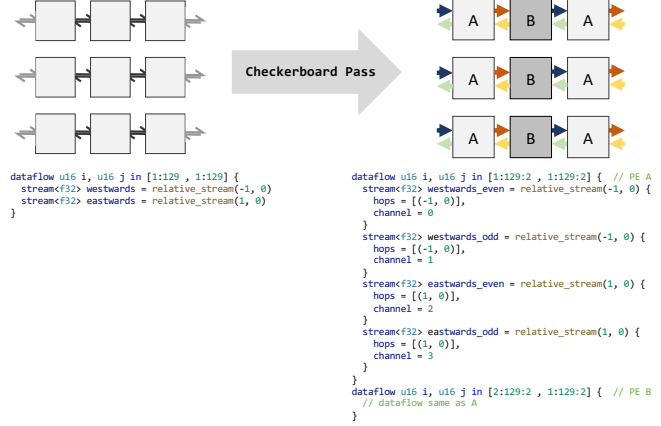


Fig. 1. Checkerboard Decomposition Pass (One Active Dimension)

```
// Input: stream s with offset (dx, dy), PE coords (i, j)
// Output: stream to use for s in the checkerboard

// Identify communication dimension
dim = (abs(dx) > 0) ? x : y
// Compute block parity based on dimension
p = (dim == x) ? (i % 2) : (j % 2)
// Determine direction bit
σ = (dx > 0 || dy > 0) ? 1 : 0
// Flip direction for receive operations
if (is_receive) σ = 1 - σ
// Select even/odd stream based on parity match
return (p == σ) ? s_even : s_odd
```

Listing 3: Stream Selection for Checkerboard Routing

operate concurrently on overlapping routes, ensuring correctness according to Section IV: *all stream edges that share a PE have different channels, there are no conflicts*.

For example, consider a stream `red` with offset $(-1, 0)$ (sending westward). When PE $(3, 0)$ sends and PE $(2, 0)$ receives, both PEs select `red_odd`, ensuring correct communication. Meanwhile, PE $(2, 0)$ sending westward selects `red_even` ($p = \sigma = 0$), preventing conflicts.

C. Task Assignment and Decomposition

In addition to color assignment, a key limited resource to utilize when creating WSE programs is tasks. Tasks can execute concurrently on a PE and the asynchrony is required to avoid deadlocks on nonblocking communication. Since SPADA is an `async-await` language, we transform the code into a CSL task graph in multiple stages, as outlined in Figure 2.

First, the `compute` block is transformed into a dependency DAG based on `completion` and `await` statements (Figure 2b). This completion DAG is then converted to a scheduling graph where every statement is explicit, containing “post” and “wait” events (Figure 2c), where synchronous statements are implemented as a post-wait sequence. The low-level statement decomposition allows us to later group them into local and data tasks according to a semantics-based rule-set (e.g., can the statement be implemented by a DSD operation).

Owing to the WSE PE architecture (Section II), task execution is constrained. In particular, a CSL program must adhere to the following constraints: (a) a local task may have up to two predecessors (triggering the task with `@activate` and

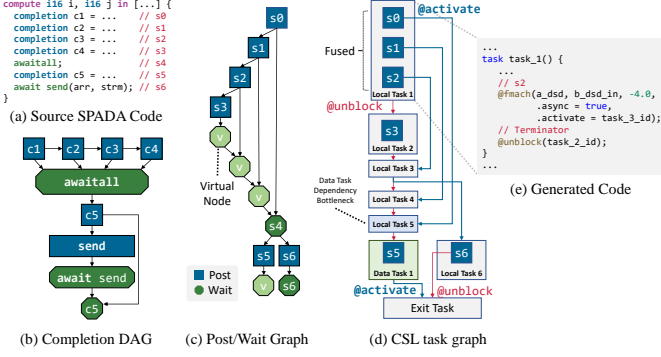


Fig. 2. SPADA-to-CSL Task Assignment Pipeline

@unblock); and (b) a data task is always active, but can be blocked (thus having one predecessor). We write a set of passes to create *virtual* nodes and local tasks to reduce the in-degree of nodes in the post/wait graph accordingly.

In the next step (Figure 2d), the post/wait graph is coarsened to tasks based on feasibility, and edges from statements to successor tasks are annotated with *activate*/*unblock*. This allows the compiler to embed the activation into an asynchronous DSD operation (see Figure 2e for an example), where a special *terminator* virtual statement can create dependencies at end of a task. One key aspect of the process is *task fusion*: a coarsening optimization pass that groups statements into CSL tasks when possible, reducing overhead and conserving valuable PE resources (namely, task IDs).

Task construction thus maintains program semantics by ensuring that operations execute in a valid topological order while maximizing opportunities for concurrent execution.

D. Code Generation

The core generation strategy partitions the spatial program into processing element (PE) rectangles, generating specialized CSL code for each such rectangle.

Automatic Vectorization. SPADA’s *foreach* and *map* constructs are particularly amenable to automatic vectorization through DSDs. The compiler employs pattern matching to identify loops that correspond to DSD operations based on type and content (e.g., *@fmac** for fused multiply-accumulate, and *@mov** for data movement). When vectorization fails, the compiler employs a tiered fallback strategy. Loop bodies satisfying purity constraints (single output, indexing-only iterator usage, no control flow) are transformed into CSL *@map* operations, where the loop body becomes a callback function with variables promoted to parameters and output assignments converted to returns. Alternatively, *foreach* loops over streams without explicit ranges become wavelet-triggered data tasks, where fabric colors trigger execution upon packet arrival. Complex control flow, non-affine indexing, or other non-conforming patterns fall back to direct CSL for-loop generation. This hierarchical approach maximizes hardware utilization through DSD operations while maintaining semantic correctness through conservative fallbacks.

Layout and Resource Allocation. The compiler also generates layout specifications that map SPADA’s abstract communication channels to physical CSL colors. A global allocation algorithm analyzes all subgrids to assign colors based on the aforementioned conflict-avoiding routing assignment. Subsequently, the compiler generates per-subgrid routing configurations with directional fabric paths, and input/output queues are assigned to the PEs’ fabric DSDs to maximize concurrency in message passing.

E. I/O Mapping

SPADA kernel arguments do not explicitly occur in *place* blocks. Therefore, an analysis pass is run on the SPADA code and the generated task graph to determine argument extents, i.e., the mapping between argument stream array indices and their corresponding PEs. The analysis collects array slice expressions and applies the *compute* subgrid to them to determine offsets. If a disjoint union of the subgrids constructs one contiguous rectangle (or one-dimensional line) across PEs, the offsets are mapped successfully. Scalar arguments are implemented in CSL as kernel function arguments that are *placed* only in PEs that use them.

To manage data transmission, the compiler determines whether to use the Cerebras memory-copy (*memcpy*) infrastructure, or whether to stream data based on kernel characteristics. Namely, *stream* arguments without an explicit buffer size or *foreach* statements without an explicit range would trigger streaming communication.

The last phase of compilation collates the aforementioned program metadata in a JSON file bundled with the compiled CSL. In turn, the SPADA Cerebras runtime uses this metadata to transmit data, benchmark, and execute kernel code.

VII. RESULTS

We run the experiments on a Cerebras WSE-2 system using CSL SDK v1.4.0. The WSE-2 chip comprises a fabric of 757×996 PEs (out of which 750×994 are usable due to the on-chip *memcpy* infrastructure). We measure each kernel 100 times and collect cycle counters from all participating PEs. The numbers reported here are median cycles of all PEs over all experiments with 95% nonparametric CI for error bars. If 95% CI is under 0.01, it is omitted for readability. For easier interpretability, we convert the number of cycles into a runtime with the formula: Runtime [μ s] = (cycles/0.85) $\cdot 10^{-3}$.

Our evaluation comprises two categories of kernels. First, we examine three hand-written SPADA kernels: blocking and pipelined reduction variants that demonstrate different algorithmic strategies, plus a copy kernel that establishes baseline memory throughput on the WSE-2. Second, we evaluate three 3D stencil kernels, originally written in GT4Py and lowered through our compilation pipeline (Sections V and VI): (1) a 2D Laplacian computing spatial derivatives in the horizontal plane, (2) a difference stencil with sequential dependencies along the vertical column direction, and (3) UVBKE, a complex momentum equation kernel from the COSMO dynamical weather core with horizontal computations. For each kernel,

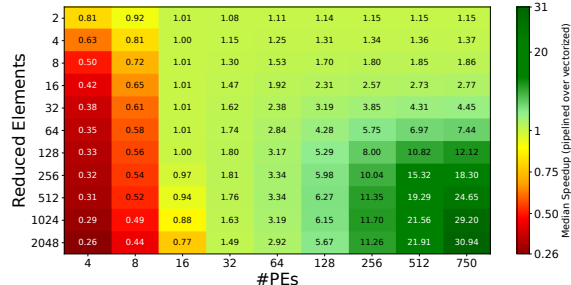


Fig. 3. Speedup of Pipelined over Vectorized 1D Reduction

we perform systematic parameter sweeps varying both spatial dimensions and PE counts to characterize performance across problem scales. All stencil experiments use $K = 80$ vertical (pressure) levels unless otherwise specified.

TABLE II
LINES OF CODE COMPARISON ACROSS REPRESENTATIONS

Kernel	GT4Py	SPADA	CSL	CSL/Source
Reduction (blocking)	—	77	636	8.26×
Reduction (pipelined)	—	91	624	6.86×
Copy	—	10	63	6.30×
Vertical Stencil	5	26	77	15.40×
2D Laplacian	4	1600	2835	708.75×
UVBKE	10	1222	2407	240.70×
Harmonic Mean	—	—	—	12.09×

A. Lines of Code Analysis

Table II compares code size across representations. Handwritten SPADA kernels require 6–8× fewer lines than equivalent CSL. For GT4Py stencils, expansion patterns reveal spatial complexity: the vertical stencil shows modest growth due to its simple sequential structure, while horizontal stencils expand dramatically—the 2D Laplacian grows from 4 lines to nearly 3000 lines of CSL—reflecting the extensive PE coordination and halo exchange logic required for distributed spatial computation.

These results validate SPADA’s dual role. As a programming language, it significantly reduces hand-written code while maintaining explicit control over performance-critical decisions. As a compiler IR, it enables tractable DSL lowering by separating domain semantics (Section V) from architecture details (Section VI), providing the abstraction boundary necessary for productive high-level programming of SDAs.

B. Reduction and Copy

Figure 3 compares pipelined versus blocking reduction performance across PE counts and data sizes. The results confirm the tradeoff identified in prior work [16]: blocking reduction excels for small configurations (up to 4× faster at 4 PEs), while pipelined reduction dominates at scale, achieving over 30× speedup with 750 PEs reducing 2048 elements. This crossover behavior demonstrates SPADA’s ability to express both variants concisely, enabling developers to select the appropriate strategy for their problem size.

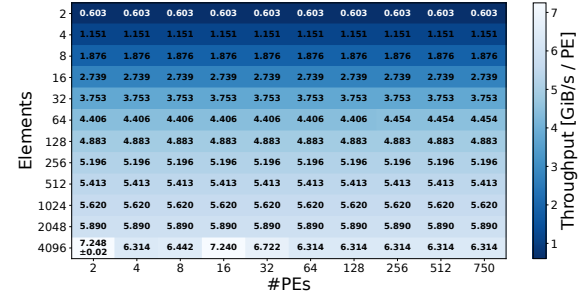


Fig. 4. Single-Precision Copy Throughput per PE (in GiB/s)

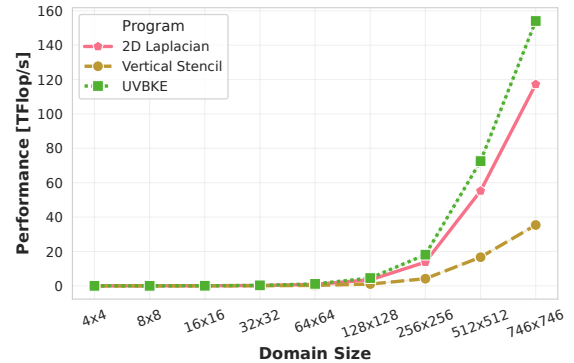


Fig. 5. Stencil Total Flop/s Performance Scaling (K=80)

Figure 4 characterizes memory throughput using a SPADA copy kernel that transfers data from device to host and back. At 4096 fp32 elements per PE, the kernel achieves 6.3–7.24 GiB/s/PE, which represents 75% - 85% of the WSE-2’s sustained memory bandwidth [18].

C. Stencil Computations

a) Performance Scaling: Figure 5 shows computational throughput across domain sizes from 4x4x80 to 746x746x80 grid points. The UVBKE kernel achieves over 150 TFlop/s at full wafer scale, while the 2D Laplacian reaches about 120 TFlop/s. More arithmetic-intense stencils achieve higher throughput. All kernels exhibit near-linear scaling with domain size, indicating low communication overhead.

Figure 6 examines performance when fixing the horizontal domain while varying the number of vertical levels. The horizontal stencils (Laplacian and UVBKE) scale well with vertical levels because each level represents independent parallel work distributed across PEs.

In contrast, the vertical stencil exhibits different behavior: throughput increases up to 17 pressure levels, then drops significantly. The initial performance gains likely result from CSL-compiler optimizations such as loop-unrolling, suggesting further improvements are possible for large sequential loops. Beyond 17 levels, however, performance drops and then remains flat because the vertical stencil’s sequential dependencies along each vertical column execute within a single PE, preventing parallelization across levels. This behavior confirms that our compiler correctly preserves algorithmic dependencies while exploiting available parallelism.

b) Weak Scaling Characteristics: Figure 7 demonstrates near-ideal weak scaling with the horizontal domain size,

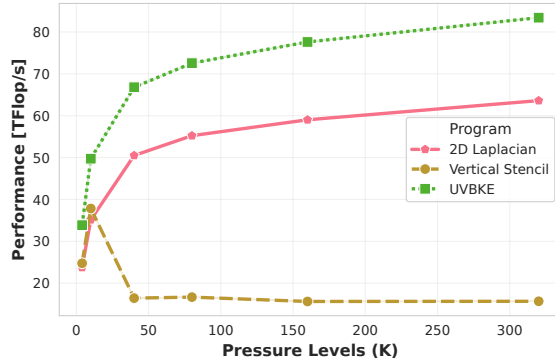


Fig. 6. Stencil Flop/s for Fixed Horizontal Domain (512×512)

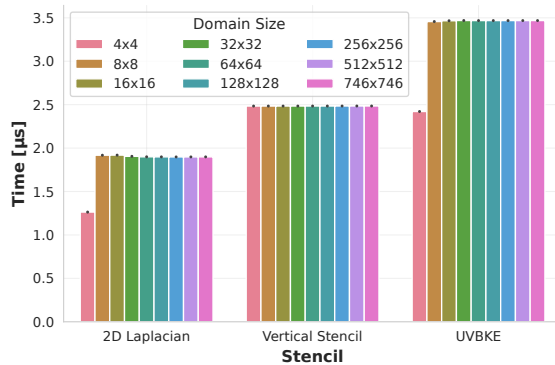


Fig. 7. Stencil Runtime vs. Horizontal Domain Size ($K=80$)

runtime remains constant (within measurement uncertainty) as both problem size and PE count increase proportionally across 3 orders of magnitude. This confirms that per-PE workload stays balanced and communication overhead remains negligible, even across the full spatial fabric. The consistency across stencil complexities validates that compiler-generated code maintains efficiency across diverse computational patterns.

D. Discussion

Our results demonstrate that SPADA significantly reduces programming complexity for spatial dataflow architectures. Developers can express complex patterns in tens of lines rather than thousands while achieving predictable performance by maximizing parallelism and arithmetic intensity.

Several optimization opportunities remain. Our checkerboard decomposition guarantees conflict-free routing but the number of colors could be further optimized. Finally, extending automatic routing beyond single-hop communication would enable efficient FFTs and multi-grid solvers. These enhancements would further improve performance while preserving SPADA’s abstraction benefits.

VIII. RELATED WORK

A. Optimizing Stencil Operations

The Open Earth Compiler [10] demonstrates multi-level IR rewriting from high-level stencil dialects through MLIR to GPU code. While sharing our focus on progressive lowering, they target GPU architectures with shared memory

and loop transformations, whereas SPADA addresses spatial dataflow architectures with distributed memory and circuit-switched routing. StencilFlow [6] maps stencil DAGs to distributed FPGA systems with automated deadlock analysis. Like SPADA, it targets spatial architectures, but differs fundamentally in targeting reconfigurable hardware with packet-switched communication rather than hardened dataflow processors requiring explicit channel assignment.

B. Computations on the Cerebras WSE

Prior work on the Cerebras WSE has demonstrated impressive performance through hand-crafted implementations [5], [12], [22], but each required extensive manual effort tailored to specific stencil patterns. Communication strategies, memory layouts, and computational kernels were tightly coupled to particular discretization schemes, and common patterns like halo exchanges had to be reimplemented for each application.

The WSE Field-equation API (WFA) [24] improved programmability with a NumPy-like interface but remains domain-specific to stencil computations on uniform Cartesian grids with fixed domain decomposition. SPADA differs in scope and design: it expresses diverse parallel patterns beyond stencils, including pipelined reductions with alternating communication and collective primitives, and serves dual roles as both a programming language and compiler IR, enabling DSL frontends like GT4Py to target spatial architectures.

Luczynski et al. [16] achieved speedups for hand-optimized reductions, requiring manual reasoning about routing conflicts across hundreds of thousands of PEs—patterns SPADA can express naturally with automatic conflict-free routing.

C. Programming Language Semantics

Our work draws on research in session types, static analysis for message-passing programs, and formal semantics for concurrent systems, while addressing unique challenges posed by spatial dataflow architectures.

Multiparty session types [5], [7], [11] enable communication safety through global-to-local projection but assume packet-switched networks with transparent routing. SPADA extends this framework with explicit routing paths and hardware channel assignment for circuit-switched NoCs with finite physical channels. *Pabble* [19] introduces parameterized session types for MPI collective operations but lacks spatial placement and routing primitives. *Bronevetsky*’s communication-sensitive dataflow [4] infers communication patterns from existing MPI code through parallel control-flow graphs. SPADA is prescriptive: explicit specification of topology, placement, and routing enables automatic routing assignment and guaranteed safety by construction—reflecting that spatial architectures require explicit data movement orchestration.

IX. CONCLUSION

SPADA demonstrates that spatial dataflow architectures can be programmed productively without sacrificing performance. By separating high-level concerns—data placement, communication patterns, and computation—from low-level

hardware details, developers can express complex parallel algorithms concisely. Our checkerboard decomposition automates conflict-free routing. The GT4Py integration validates SPADA’s role as both programming language and compiler IR, enabling domain scientists to target spatial architectures through familiar interfaces.

While spatial dataflow platforms like Cerebras excel at AI workloads, programming them for broader HPC applications has remained prohibitively difficult. SPADA changes this by providing a principled programming model accessible to diverse algorithmic patterns, unleashing spatial architecture performance across the full spectrum of HPC workloads.

SPADA’s intermediate representation provides a foundation for systematic optimization passes while dramatically lowering the barrier for porting new applications. Where hand-coding previously required weeks, SPADA enables rapid exploration of diverse workloads. This positions spatial dataflow computing as a viable platform across the breadth of high-performance scientific computing.

ACKNOWLEDGMENTS

Work by Lawrence Livermore National Laboratory was performed under the auspices of the U.S. Department of Energy under contract DE-AC52-07NA27344 (LLNL-CONF-2012380).

Generative AI was used to improve the language and overall presentation of this paper [2].

REFERENCES

- [1] ADVE, S. V., AND HILL, M. D. Weak ordering - A new definition. In *Proceedings of the 17th Annual International Symposium on Computer Architecture, Seattle, WA, USA, June 1990* (1990), J. Baer, L. Snyder, and J. R. Goodman, Eds., ACM, pp. 2–14.
- [2] ANTHROPIC. Sonnet 4.5, 2025.
- [3] BEN-NUN, T., GRONER, L., DECONINCK, F., WICKY, T., DAVIS, E., DAHM, J., ELBERT, O., GEORGE, R., MCGIBBON, J., TRÜMPER, L., WU, E., FUHRER, O., SCHULTHESS, T. C., AND HOEFLER, T. Productive performance engineering for weather and climate modeling with python. In *SC22: International Conference for High Performance Computing, Networking, Storage and Analysis, Dallas, TX, USA, November 13-18, 2022* (2022), F. Wolf, S. Shende, C. Culhane, S. R. Alam, and H. Jagode, Eds., IEEE, pp. 73:1–73:14.
- [4] BRONEVETSKY, G. Communication-sensitive static dataflow for parallel message passing applications. In *Proceedings of the CGO 2009, The Seventh International Symposium on Code Generation and Optimization, Seattle, Washington, USA, March 22-25, 2009* (2009), IEEE Computer Society, pp. 1–12.
- [5] CASTRO-PEREZ, D., FERREIRA, F., GHERI, L., AND YOSHIDA, N. Zood: a DSL for certified multiparty computation: from mechanised metatheory to certified multiparty processes. In *PLDI ’21: 42nd ACM SIGPLAN International Conference on Programming Language Design and Implementation, Virtual Event, Canada, June 20-25, 2021* (2021), S. N. Freund and E. Yahav, Eds., ACM, pp. 237–251.
- [6] DE FINE LICHT, J., KUSTER, A., MATTEIS, T. D., BEN-NUN, T., HOFER, D., AND HOEFLER, T. Stencilflow: Mapping large stencil programs to distributed spatial computing systems. In *IEEE/ACM International Symposium on Code Generation and Optimization, CGO 2021, Seoul, South Korea, February 27 - March 3, 2021* (2021), J. W. Lee, M. L. Soffa, and A. Zaks, Eds., IEEE, pp. 315–326.
- [7] DENIÉLOU, P., AND YOSHIDA, N. Multiparty compatibility in communicating automata: Characterisation and synthesis of global session types. In *Automata, Languages, and Programming - 40th International Colloquium, ICALP 2013, Riga, Latvia, July 8-12, 2013, Proceedings, Part II* (2013), F. V. Fomin, R. Freivalds, M. Z. Kwiatkowska, and D. Peleg, Eds., vol. 7966 of *Lecture Notes in Computer Science*, Springer, pp. 174–186.
- [8] DEY, N., GOSAL, G., CHEN, Z., KHACHANE, H., MARSHALL, W., PATHRIA, R., TOM, M., AND HESTNESS, J. Cerebras-gpt: Open compute-optimal language models trained on the cerebras wafer-scale cluster. *CoRR abs/2304.03208* (2023).
- [9] GOPALAKRISHNAN, G., KIRBY, R. M., SIEGEL, S. F., THAKUR, R., GROPP, W., LUSK, E. L., DE SUPINSKI, B. R., SCHULZ, M., AND BRONEVETSKY, G. Formal analysis of mpi-based parallel programs. *Commun. ACM* 54, 12 (2011), 82–91.
- [10] GYSI, T., MÜLLER, C., ZINENKO, O., HERHUT, S., DAVIS, E., WICKY, T., FUHRER, O., HOEFLER, T., AND GROSSER, T. Domain-specific multi-level IR rewriting for GPU: the open earth compiler for gpu-accelerated climate simulation. *ACM Trans. Archit. Code Optim.* 18, 4 (2021), 51:1–51:23.
- [11] HONDA, K., YOSHIDA, N., AND CARBONE, M. Multiparty asynchronous session types. In *Proceedings of the 35th ACM SIGPLAN-SIGACT Symposium on Principles of Programming Languages, POPL 2008, San Francisco, California, USA, January 7-12, 2008* (2008), G. C. Necula and P. Wadler, Eds., ACM, pp. 273–284.
- [12] JACQUELIN, M., ARAYA-POLO, M., AND MENG, J. Scalable distributed high-order stencil computations. In *SC22: International Conference for High Performance Computing, Networking, Storage and Analysis, Dallas, TX, USA, November 13-18, 2022* (2022), F. Wolf, S. Shende, C. Culhane, S. R. Alam, and H. Jagode, Eds., IEEE, pp. 30:1–30:13.
- [13] KUNDU, Y., KAUR, M., WIG, T., KUMAR, K., KUMARI, P., PURI, V., AND ARORA, M. A comparison of the cerebras wafer-scale integration technology with nvidia gpu-based systems for artificial intelligence. *CoRR abs/2503.11698* (2025).
- [14] LAMPORT, L. Time, clocks, and the ordering of events in a distributed system. *Commun. ACM* 21, 7 (1978), 558–565.
- [15] LIE, S. Inside the cerebras wafer-scale cluster. *IEEE Micro* 44, 3 (2024), 49–57.
- [16] LUCZYNSKI, P., GIANINAZZI, L., IFF, P., WILSON, L., SENSI, D. D., AND HOEFLER, T. Near-optimal wafer-scale reduce. In *Proceedings of the 33rd International Symposium on High-Performance Parallel and Distributed Computing, HPDC 2024, Pisa, Italy, June 3-7, 2024* (2024), P. Dazzi, G. Mencagli, D. K. Lowenthal, and R. M. Badia, Eds., ACM, pp. 334–347.
- [17] MANSON, J., PUGH, W. W., AND ADVE, S. V. The java memory model. In *Proceedings of the 32nd ACM SIGPLAN-SIGACT Symposium on Principles of Programming Languages, POPL 2005, Long Beach, California, USA, January 12-14, 2005* (2005), J. Palsberg and M. Abadi, Eds., ACM, pp. 378–391.
- [18] MIYAJIMA, T., MATSUZAKI, R., AND FUKUOKA, L. STREAM benchmark on Cerebras Wafer-Scale Engine-2. Poster presented at ISC High Performance 2024, May 2024. May 13–15, 2024.
- [19] NG, N., AND YOSHIDA, N. Pabble: Parameterised scribble for parallel programming. In *22nd Euromicro International Conference on Parallel, Distributed, and Network-Based Processing, PDP 2014, Torino, Italy, February 12-14, 2014* (2014), IEEE Computer Society, pp. 707–714.
- [20] ORENES-VERA, M., SHARAPOV, I., SCHREIBER, R., JACQUELIN, M., VANDERMERSCH, P., AND CHETLUR, S. Wafer-scale fast fourier transforms. In *Proceedings of the 37th International Conference on Supercomputing, ICS 2023, Orlando, FL, USA, June 21-23, 2023* (2023), K. A. Gallivan, E. Gallopoulos, D. S. Nikolopoulos, and R. Beivide, Eds., ACM, pp. 180–191.
- [21] PAREDES, E. G., GRONER, L., UBBIALI, S., VOGT, H., MADONNA, A., MARIOTTI, K., CRUZ, F. A., BENEDICIC, L., BIANCO, M., VANDEVONDELE, J., AND SCHULTHESS, T. C. Gt4py: High performance stencils for weather and climate applications using python. *CoRR abs/2311.08322* (2023).
- [22] SAI, R., JACQUELIN, M., HAMON, F. P., ARAYA-POLO, M., AND SETTGAST, R. R. Massively distributed finite-volume flux computation. In *Proceedings of the SC ’23 Workshops of The International Conference on High Performance Computing, Network, Storage, and Analysis, SC-W 2023, Denver, CO, USA, November 12-17, 2023* (2023), ACM, pp. 1713–1720.
- [23] TROTTER, M. V., NGUYEN, C. Q., YOUNG, S., WOODRUFF, R. T., AND BRANSON, K. M. Epigenomic language models powered by cerebras. *CoRR abs/2112.07571* (2021).
- [24] WOO, M., JORDAN, T., SCHREIBER, R., SHARAPOV, I., MUHAMMAD, S., KONERU, A., JAMES, M., AND ESENDELFT, D. V. Disruptive changes in field equation modeling: A simple interface for wafer scale engines. *CoRR abs/2209.13768* (2022).